Crystallography Reports, Vol. 44, No. 4, 1999, pp. 565–574. Translated from Kristallografiya, Vol. 44, No. 4, 1999, pp. 612–622.
Original Russian Text Copyright © 1999 by Pushcharovskii, Pekov, Pluth, Smith, Ferraris, Vinogradova, Arakcheeva, Soboleva, Semenov.

STRUCTURE OF INORGANIC, ORGANIC, AND MACROMOLECULAR COMPOUNDS. CRYSTAL CHEMISTRY

Raite, Manganonordite-(Ce), and Ferronordite-(Ce) from the Lovozero Massif: Crystal Structures and Mineralogical Geochemistry

D. Yu. Pushcharovskii*, I. V. Pekov*, J. Pluth, J. Smith**, G. Ferraris***, S. A. Vinogradova*, A. V. Arakcheeva****, S. V. Soboleva***, and E. I. Semenov*******

** Moscow State University, Vorob'evy gory, Moscow, 119899 Russia*

*** University of Chicago, USA*

**** University of Turin, Italy*

***** Baikov Institute of Metallurgy, Russian Academy of Sciences, Leninskii pr. 49, Moscow, 117334 Russia*

****** Fersman Mineralogical Museum, Russian Academy of Sciences, Leninskii pr. 18, Moscow, 117071 Russia*

Received January 22, 1998

Abstract—The structures of three minerals discovered recently in alkaline rocks of Lovozero pegmatites have been determined. The structure and composition of raite $Na_3Mn_3Ti_{0.25}[Si_2O_5]_4(OH)_2 \cdot 10H_2O$ are refined using a crystal with an effective size of 6 μm (synchrotron radiation). It is found that the unit cell of the mineral is monoclinic and not orthorhombic. Comparison of raite with structurally related minerals makes it possible to describe its structure on the basis of the modular theory of crystal structures. The structures of two new representatives of the nordite mineralogical family, namely, ferronordite-(Ce) and manganonordite-(Ce), are refined. These minerals are described by the general formula $Na_3SrTRM^{2+}Si_6O_{17}$ with *TR* being predominantly Ce-cations, and M^{2+} being predominantly Fe^{2+} and Mn^{2+} in ferronordite-(Ce) and manganonordite-(Ce), respectively. The silicate ribbons in nordite are topologically comparable with those in vlasovite and haiweeite. New Mn-silicates found in high-alkaline rocks from different areas and the results of structural studies make it possible to reveal crystal-chemical features associated with their crystallogenesis.

The number of terrestrial minerals discovered to date approaches 4000, and the list is annually supplemented with 40–50 mineral species. However, approximately 20% of minerals have not yet been structurally studied because of small sizes and imperfection of their crystals. The application of new modern approaches to structural studies, as well as increasing structural possibilities, can be a help in decreasing the number of minerals, whose structures remain unknown, thus extending the knowledge of forms of concentrating chemical elements in the Earth's crust, relations between different structural types, and other topical aspects of crystal chemistry and mineralogy. In this respect, structural studies of Na,Mn-silicate raite, which was found in 1973 as extraordinarily thin (up to 0.02–0.04 mm) needle-like crystals, and two new minerals, manganonordite-(Ce) and ferronordite-(Ce), discovered in 1997 were of interest because they made it possible to reveal the characteristic features of mineralogical geochemistry of the Lovozero alkaline massif.

Raite. Raite, which was originally described by the $Na_4Mn_3Si_8(O,OH)_{24} \cdot H_2O$ formula, was discovered in the Yubileinaya pegmatite lode [1] located within a layered complex of high-alkaline (agpaitic) rocks at the Karnasurt mountain of the Lovozero alkaline massif (the Kola Peninsula). The orthorombic unit cell parameters [a = 30.6(1) Å, b = 5.31(2) Å, c = 18.20(5) Å, space group $C222_1$] were determined from X-ray diffraction oscillation patterns and Weissenberg's X-ray photographs (moving crystal and film technique) [1]. A single crystal (3 × 3 × 65 μm) selected for X-ray diffraction study was glued on a 1-μm-thick glass fiber mounted on a diffractometer at the European Synchrotron Radiation Facility (ESFR, Grenoble, France). The monochromated X-ray beam (λ = 0.6883 Å) was focused with two elliptic mirrors to 30 μm. A Si(111) crystal cooled with liquid nitrogen was used as a monochromator. One-half of the crystal volume (~300 μm^3) was subjected to radiation.

X-ray diffraction data (6599 non-zero reflections) were collected with the use of a position-sensitive detector (CCD; a 11-cm-diameter fluorescent screen) at 73 orientations of the crystal rotated around φ; 10°-rotation frames were exposed for 20 s each. The monoclinic unit cell parameters [a = 15.1(1) Å, b = 17.6(1) Å, c = 5.290(4) Å, β = 100.5(2)°, V = 1382.33 $Å^3$, space group $C2/m$] differ substantially from those reported in [1]. The structure was solved and refined with the SHELXTL program [2] using 1164 independent reflections (R_{int} = 0.05) to R_{hkl} = 0.067 [R_{hkl} = 0.059 for 916 reflections with $F_0 > 4\sigma(F_0)$]. Only 325 of 3080 reflec-

1063-7745/99/4404-0565$15.00 © 1999 МАИК "Наука/Interperiodica"

Table 1. Coordinates and thermal parameters of the basis atoms in the structure of raite

Atom	*x/a*	*y/b*	*c/z*	U_{eq}, Å^2
Mn(1)	0.0	0.0	0.0	0.013(1)
Mn(2)	0.5	0.40289(8)	0.5	0.017(1)
Na(1)	0.5	0.2997(2)	0.0	0.019(2)
Na(2)	0.5	0.0	0.0	0.040(3)
Ti*	0.5	0.204(1)	0.5	0.025(8)
Si(1)	0.3121(1)	0.41406(9)	0.0569(5)	0.010(1)
Si(2)	0.3052(1)	0.32828(9)	0.5497(5)	0.011(1)
O(1)	0.4198(3)	0.4133(2)	0.118(1)	0.016(2)
O(2)	0.0882(3)	0.1816(3)	0.408(1)	0.021(2)
O(3)	0.25	0.25	0.5	0.028(3)
O(4)**	0.0678(5)	0.0	0.361(2)	0.020(3)
O(5)	0.2718(4)	0.5	0.006(2)	0.012(3)
O(6)	0.2295(3)	0.1328(3)	0.204(1)	0.013(2)
O(7)	0.2686(3)	0.3802(3)	0.294(1)	0.014(2)
O(8)***	0.4018(6)	0.0	0.304(2)	0.042(4)
O(9)***	0.0720(5)	0.3992(4)	0.271(2)	0.054(3)
O(10)***	0.4176(6)	0.2096(4)	0.201(2)	0.062(4)

* The occupancy factor of the Ti position is 0.125(4).
** OH.
*** H_2O.

Table 2. Interatomic distances (Å) in the structure of raite

Mn(1) octahedron		Mn(2) octahedron	
Mn(1)–O(4)	2.00(1) × 4	Mn(2)–O(2)	2.11(1) × 2
O(1)	2.112(9) × 2	O(1)	2.164(8) × 2
		O(4)	2.186(8) × 2
Na(1) octahedron		**Na(2) octahedron**	
Na(1)–O(2)	2.342(9) × 2	Na(2)–O(8)	2.38(1) × 2
O(10)	2.38(1) × 2	O(9)	2.41(1) × 4
O(1)	2.48(1) × 2		
Ti octahedron			
Ti–O(10)		1.83(1) × 2	
O(9)		2.53(2) × 2	
O(2)		2.51(2) × 2	
Si(1) tetrahedron		**Si(2) tetrahedron**	
Si(1)–O(1)	1.60(1)	Si(2)–O(2)	1.59(1)
O(7)	1.628(7)	O(3)	1.607(7)
O(1)	1.631(7)	O(6)	1.642(7)
O(1)	1.634(9)	O(7)	1.645(7)
	⟨1.623⟩		⟨1.621⟩
O(1)–O(7)	2.531(5)	O(2)–O(3)	2.767(4)
O(6)	2.939(5)	O(6)	2.540(5)
O(5)	2.770(6)	O(7)	2.890(5)
O(7)–O(6)	2.640(1)	O(3)–O(6)	2.609(4)
O(5)	2.600(7)	O(7)	2.553(4)
O(6)–O(5)	2.587(6)	O(7)–O(6)	2.640(1)
	⟨2.678⟩		⟨2.666⟩

tions forbidden according to the *C* centering had small intensities with $I \geq 1\ \sigma(I)$. However, the refinement in space group *P*2/*m* confirmed the model based on the *C*-centered cell.

The composition of raite crystals was confirmed by the results of qualitative electron microprobe analysis (Cameca SX-50), which revealed the presence of Mn, Na, Si, and a small amount of Ti. The maximum of the electron density observed at the final stage of the refinement was identified with a partial occupancy (~12%) of the Ti sites. Calculations of the balance of bond valences around the anions made it possible to distinguish O, OH, and H_2O among the sites of O atoms. As a result, the chemical formula of raite was found to be $Na_3Mn_3Ti_{0.25}[Si_2O_5]_4(OH)_2 \cdot 10H_2O$ ($Z = 2$, $F(000) = 974$, $\rho_{calcd} = 2.39$ g/cm^3, $\rho_{exp} = 2.39(2)$ g/cm^3). The final difference Fourier synthesis contained no noticeable maxima: $\Delta\rho_{max} = 0.98\ e/Å^3$ and $\Delta\rho_{min} = -0.82\ e/Å^3$. The structural model was tested using the MISSYM program [3], which did not reveal pseudosymmetry elements.

The atomic coordinates and interatomic distances are given in Tables 1 and 2, respectively. Calculations of the theoretical X-ray diffraction pattern [4] demonstrated that it is in complete agreement with the X-ray powder data [1]. Below are given the values d_{exp}, d_{calcd}; I_{exp}, and I_{calcd}, respectively, for five strongest reflections: (1) 11.4, 11.35, 10, and 100; (2) 4.5, 4.48, 8, and 12; (3) 3.8, 3.79 + 3.78, 6, and 8; (4) 2.939, 2.928, 10, and 10; and (5) 2.65, 2.632, 10, and 17.

The most distinguishing feature of the structure is the presence of the silicon–oxygen layers $[Si_2O_5]$ (Fig. 1). The orientations of the $[SiO_4]$ tetrahedra change every two chains, which are parallel to [001]. Analogous (Si,O) layers are observed in the structures of palygorskite $Mg_5[Si_2O_5]_4(OH)_2 \cdot 8H_2O$ [5] and yofortierite $Mn_5[Si_2O_5]_4(OH)_2 \cdot 8H_2O$ [6]. Octahedral ribbons, which are parallel to [001] and consist of alternating units of two Mn(2) octahedra and three Na(1)–Mn(1)–Na(1) octahedra, are located between terminal vertices of Si tetrahedra facing each other (Fig. 2). These octahedral ribbons (Fig. 3) can be considered as relics of micaceous octahedral layers. According to [7],

these layers are broken into ribbons if the size of octahedral complexes is substantially larger than that of tetrahedral complexes. The incorporation of bulky $[Na(1)(O,OH,H_2O)_6]$ octahedra into octahedral ribbons leads to an increase in the size inconsistency. As a result, not only octahedral layers are broken, but tetrahedral (Si,O) layers are bent as well.

The structure of intersillite $(Na,K)Mn(Ti,Nb)Na_5(O,OH)(OH)_2[Si_{10}O_{23}(O,OH)_2] \cdot 4H_2O$ contains Na octahedra as elements of octahedral ribbons contacting with (Si,O) layers [8]. However, in the latter case, nature finds another way for decreasing the strain of this contact by forming topologically different inverse (Si,O) layers from eight-membered, six-membered, and five-membered rings. Another Na,Mn-silicate, varennesite $Na_8Mn_2[Si_{10}O_{25}](OH,Cl)_2 \cdot 12H_2O$ [9], is all the more similar in composition to raite. The tetrahedral networks in this mineral involve ten-membered, six-membered, and four-membered rings; in this case, the inversion of the orientation of the Si tetrahedra is observed in the six-membered rings linked in pairs.

Comparison of the tetrahedral layers in the structurally studied Na,Mn-silicates (varennesite, intersillite, and raite) confirmed the conclusion [7] that the configuration of (Si,O) networks is governed by the radius of octahedrally coordinated cations (r_M) and by the ratio between octahedrally and tetrahedrally coordinated cations (n_M/n_t). The values of r_M are 1, 0.945, and 0.915 and the values of n_M/n_t are 1, 0.80, and 0.78 for varennesite, intersillite, and raite, respectively. Consequently, an increase in these parameters is accompanied by the redistribution of six-membered rings in tetrahedral layers to form bulkier ten-membered rings in varennesite.

The relation between raite and other layered silicates is determined by the difference in the inversion of tetrahedra in (Si,O) layers. In sepiolite, this inversion is repeated every three chains with a period of two tetrahedra, whereas intersillite is characterized by different orientations of tetrahedra of the six-membered and, in part, eight-membered rings. Amphibole likite $Na(Na,Ca)_2(Mg,Fe^{3+},Mn^{3+},Al,Li)_5(Si_4O_{11})$ [8] can be also classed with these silicates.

The similarity of the compositions and unit-cell parameters of raite and palygorskite, on the one hand, and kalifersite $(K,Na)_5Fe_7^{3+}[Si_{20}O_{50}](OH)_6 \cdot 12H_2O$, which was discovered recently in the hydrothermolite of the Khibiny alkaline massif (the Kola Peninsula), on the other hand, was noted in [10]. This gave grounds to propose the model of kalifersite structure built up of alternating palygorskite-like and sepiolite-like elements, which give rise to (Si,O) layers with the inversion of tetrahedra (Fig. 4). Therefore, the structures of raite, palygorskite, kalifersite, and sepiolite can be considered as members of a polysomatic series P_PS_S, which go under the general name "sepioles" (by analogy with "biopyriboles"). In the P_PS_S symbol, P and S denote the

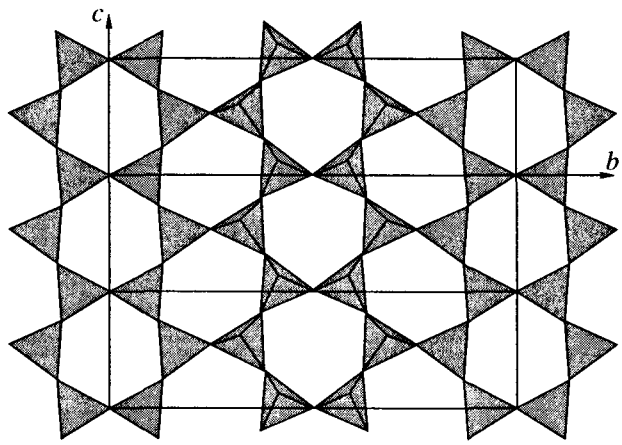

Fig. 1. A fragment of the silicon–oxygen layers $[Si_2O_5]$ parallel to (100) in the structure of raite.

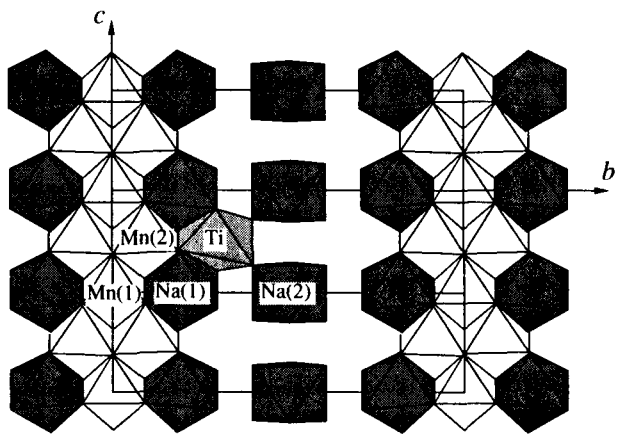

Fig. 2. Octahedral layers in the structure of raite. Ribbons formed from Mn octahedra and Na(1) octahedra are extended along [001]. Isolated Na(2) octahedra are linked to ribbons via distorted Ti octahedra statistically occupied (the occupancy is 0.125).

palygorskite and sepiolite fragments, respectively. Therefore, raite and kalifersite are specified by P_1S_0 and P_1S_1, respectively. In addition, if the statistical distribution of Ti octahedra in the structure of raite is ignored, infinite layers of cationic polyhedra located between tetrahedral silicon–oxygen networks are common to both structures. In this respect, the structures of raite and kalifersite can be considered as intermediate between usual layered silicates containing three-layer stacks and silicates containing layers, which are characterized by the inverse orientation of tetrahedra and whose octahedral wall are broken into ribbons.

Comparison of the structures of raite and palygorskite demonstrated that both structures are based on mixed frameworks, namely, $\{Na_2Mn_3^{2+}[Si_2O_5]_4(OH)_2\}^{2+}$ in raite and

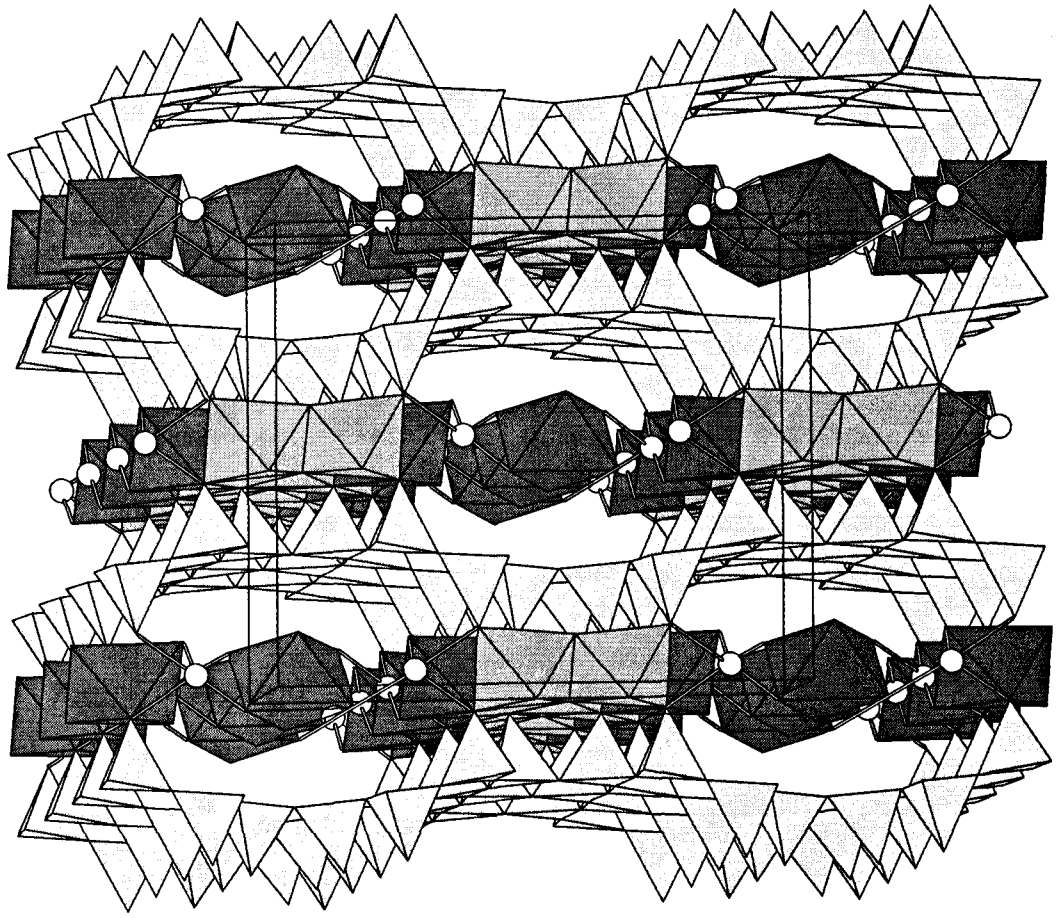

Fig. 3. Stereoview of the structure of raite. Empty circles denote Ti atoms, the dark and pale hatchings indicate Na and Mn octahedra, respectively.

$\{Mg_5[Si_2O_5]_4(OH)_2\}$ in palygorskite. In raite, channels extended along [001] are filled with columns of isolated $[Na(OH,H_2O)_6]$ octahedra, whereas in palygorskite, these channels accommodate only water molecules. In raite, Ti cations, which partially occupy their sites and are located in distorted octahedra, are responsible for weak bonds between clathrate Na(2) octahedra and the mixed framework. Therefore, the structural formula of raite can be represented as follows: $\{Na_2Mn_3^{2+}[Si_2O_5]_4(OH)_2(H_2O)_4\}^{2-}\{Ti_{0.25}^{4+}Na(H_2O)_6\}^{2+}$.

Manganonordite-(Ce) and ferronordite-(Ce). Minerals of the nordite family of the general formula $Na_3SrTRM^{2+}Si_6O_{17}$ are characterized by a broad spectrum of isomorphism, which extends to positions M^{2+} = Zn, Mn, Fe, or Mg and TR = Ce or La. The structure of nordite was first studied using a sample containing Ce as the predominant rare-earth cation and Zn as the predominant M^{2+} cation [11]. This study demonstrated that the nordite structure is characterized by mixed tetrahedral layers of the silicon–oxygen $[Si_6O_{17}]$ ribbons and M^{2+} tetrahedra, which are linked to slabs of bulky Sr, Ce, and Na polyhedra. Subsequently, this motif was refined after the determination of the structure of the La,Zn-analog [12]. More accurate estimates of interatomic distances in the Na polyhedra and of the content of these polyhedra made it possible to take a somewhat different view of the topology of the overall slab formed from bulky cationic polyhedra.

In 1997, the nordite family was supplemented with two new representatives, namely, with manganonordite-(Ce) and ferronordite-(Ce). A distinguishing feature of these minerals is a predominance of Ce in TR positions and a predominance of Mn and Fe in M^{2+} positions in manganonordite-(Ce) and ferronordite-(Ce), respectively. Structural studies of these minerals were of particular interest because the results obtained refined an understanding of the correlation between the composition and the structure for representatives of the nordite family.

Manganonordite-(Ce) and ferronordite-(Ce) were found in ultraagpaitic formations from the Lovozero alkaline massif. The chemical compositions of both minerals were determined by electron microprobe

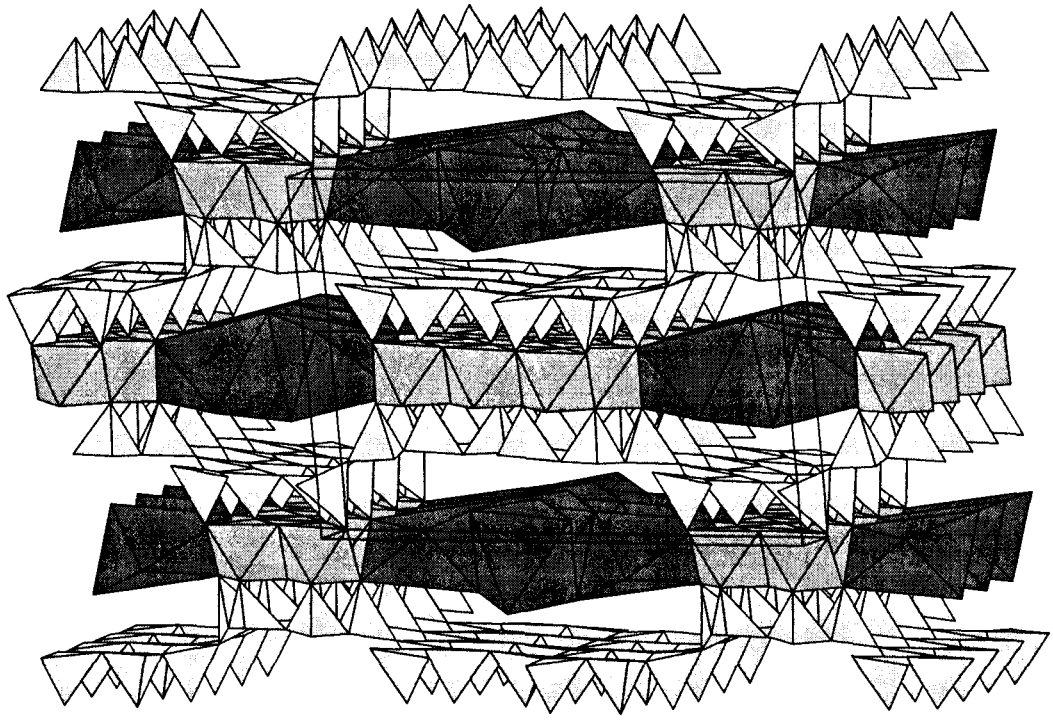

Fig. 4. Stereoview of the structure of kalifersite. The pale hatching indicates Fe octahedra, the dark hatching indicates (K,Na) polyhedra.

analysis (Cameca SX 50):

$$\text{manganonordite-(Ce)}(Na_{2.96}Ca_{0.05})_{\Sigma 3.0} \times (Si_{1.02}Ba_{0.02})_{\Sigma 1.04}(Ce_{0.51}La_{0.42}Nd_{0.05}Pr_{0.02})_{\Sigma 1.00} \times (Mn_{0.42}Zn_{0.24}Fe_{0.23}Mg_{0.10})_{\Sigma 0.99}Si_{5.97}O_{17};$$

and ferronordite-(Ce)

$$(Na_{2.91}Ca_{0.10})_{\Sigma 3.01}(Sr_{0.97}Ba_{0.02})_{\Sigma 0.99} \times (Ce_{0.52}La_{0.43}Nd_{0.04}Pr_{0.03})_{\Sigma 1.02} \times (Fe_{0.41}Mn_{0.25}Zn_{0.22}Mg_{0.10})_{\Sigma 0.98}Si_{5.97}O_{17}.$$

The unit-cell parameters and characteristics of the refinement of both structures are given in Table 3. The atomic coordinates are listed in Tables 4 and 5. Interatomic distances are presented in Tables 6 and 7.

The structures of both minerals retain all principal features of the nordite structural type. These are primarily the $[Si_6O_{17}]$ ribbons parallel to [001], which are linked into mixed tetrahedral layers of eight-membered, five-membered, and four-membered rings via tetrahedra of divalent cations (Fig. 5). Cyclic branched tetrahedral $[Si_6O_{17}]$ ribbons are commonly considered as elements formed by the $[Si_4O_{12}]$ four-membered rings linked to each other via $[Si_2O_7]$ diortho groups. The structure of vlasovite $Na_2Zr[Si_4O_{11}]$ [13] consists of the topologically similar $[Si_4O_{11}]$ ribbons of four-membered rings, which are directly linked to each other, whereas the structure of uranyl silicate haiweeite $Ca(UO_2)[Si_5O_{12}(OH)_2] \cdot 5H_2O$ studied recently [14] contains topologically similar $[Si_4O_{11}]$ ribbons formed from four-membered rings linked via isolated tetrahedra. Comparison of the structures of Zn-, Fe-, and Mn-nordites demonstrated that the size of the M^{2+} tetrahedron increases as the average ionic radius of the divalent cation (which was calculated taking into account the real occupancy of this position in accordance with the chemical composition) increases in this series. Indeed, in Zn-nordite [12], $\langle rM^{2+}\rangle$ is 0.606 Å and the average $\langle M\text{–O}\rangle$ and $\langle \text{O–O}\rangle$ distances in the M^{2+} tetrahedron are 1.95 and 3.18 Å, respectively. In ferronordite-(Ce), in which $\langle rM^{2+}\rangle$ is 0.612 Å, the corresponding values are 1.981 and 3.197 Å, respectively. In manganonordite-(Ce), in which $\langle rM^{2+}\rangle$ is 0.623 Å, the M^{2+}–O and $\langle \text{O–O}\rangle$ distances are 1.988 and 3.244 Å, respectively.

Mixed tetrahedral layers alternate with layers of bulky Sr, *TR*, and Na polyhedra along [010]. As a result, the structural type of nordite is comparable with the structures of the datolite–gadolinite family [15]. The similarity of both structural types is accented by the close values of the unit-cell parameters. Actually, for representatives of the datolite–gadolinite family, the parameters of the unit cell in the plane of the tetrahedral networks and polyhedral layers are half as large as those in nordites (~9.8 and ~7.6 Å), and the third parameter is similar to that in nordites (~5 Å).

We refined both structures with the use of substantially larger numbers of reflections (compared to those used by Sokolova *et al.* [12]), which made it possible to improve the accuracy of the interatomic distances determined in all the coordination polyhedra. The results of our investigations confirmed the conclusion

Table 3. Main crystal data and refinement results for ferronordite-(Ce) and manganonordite-(Ce)

Mineral	Ferronordite-(Ce)	Manganonordite-(Ce)
Diffractometer	Syntex $P\bar{1}$	Syntex $P\bar{1}$
λ, Å	0.71069	0.71069
Radiation	MoK_α	MoK_α
Monochromator	Graphite	Graphite
Crystal size	0.5 × 0.25 × 0.15 mm	0.4 × 0.2 × 0.1 mm
Crystal system	Orthorhombic	Orthorhombic
Space group	*Pcca*	*Pcca*
Unit-cell parameters	a = 14.46(1) Å	a = 14.44(2) Å
	b = 5.194(3) Å	b = 5.187(5) Å
	c = 19.874(9) Å	c = 19.82(1) Å
V, Å^3	1492.39, 4	1485.10, 4
$(\sin\theta/\lambda)_{max}$, Å^{-1}	1.08	1.10
No. of measured reflections	4016	5265
No. of observed reflections	3803	3534
No. of reflections with $I > 3\sigma(I)$	3623	3433
Program package used in calculations	AREN	AREN
Program used for applying absorption corrections	DIFABS	DIFABS
μ, cm^{-1}	80.5	80.6
R_{iso}	0.062	0.059
R_{aniso}	0.054	0.044

Table 4. Coordinates and thermal parameters of the basis atoms in the structure of manganonordite-(Ce)

Atom	Occupancy	*x/a*	*y/b*	*z/c*	B_{iso}, Å^2
Sr	0.981 Sr + 0.019 Ba	0.25	0.0	0.02227(2)	0.173(6)
Mn	0.42 Mn + 0.24 Zn + 0.1 Mg + 0.23 Fe	0.25	0.5	0.17012(4)	0.18(1)
Ce	0.52 Ce + 0.43 La + 0.05 Nd	0.25	0.0	0.31981(1)	0.098(4)
Si(1)	1.0 Si	0.09814(8)	0.4616(2)	0.06430(6)	0.02(2)
Si(2)	1.0 Si	0.10170(9)	0.5424(2)	0.27472(6)	0.01(1)
Si(3)	1.0 Si	0.11141(8)	0.5459(2)	−0.08130(6)	0.01(1)
Na(1)	0.983 Na + 0.017 Ca	0.0	0.0	0.0	0.82(4)
Na(2)	0.983 Na + 0.017 Ca	0.0697(2)	0.0093(6)	0.1714(1)	1.10(4)
O(1)	1.0 O	0.9948(2)	0.3374(6)	0.0819(1)	0.18(3)
O(2)	1.0 O	0.1703(2)	0.2990(6)	0.1085(1)	0.30(4)
O(3)	1.0 O	0.1179(2)	0.3567(6)	−0.0147(1)	0.17(4)
O(4)	1.0 O	0.1026(2)	0.7653(6)	0.0675(1)	0.40(4)
O(5)	1.0 O	0.0	0.6441(9)	0.25	0.40(6)
O(6)	1.0 O	0.1758(2)	0.7154(6)	0.2340(1)	0.24(4)
O(7)	1.0 O	0.1170(2)	0.6503(6)	0.3533(1)	0.24(4)
O(8)	1.0 O	0.1151(2)	0.2404(7)	0.2720(1)	0.48(4)
O(9)	1.0 O	0.1853(2)	0.2299(6)	0.4181(1)	0.37(4)

Table 5. Coordinates and thermal parameters of the basis atoms in the structure of ferronordite-(Ce)

Atom	Occupancy	*x/a*	*y/b*	*z/c*	B_{iso}, Å^2
Sr	0.98 Sr + 0.02 Ba	0.25	0.0	0.0226(1)	0.87(1)
Fe	0.42 Fe + 0.26 Mn + 0.22 Zn + 10 Mg	0.25	0.5	0.1700(1)	0.68(1)
Ce	0.51 Ce + 0.42 La + 0.04 Nd + 0.03 Pr	0.25	0.0	0.3199(1)	0.57(1)
Si(1)	1.0 Si	0.0983(1)	0.4623(2)	0.0643(1)	0.48(1)
Si(2)	1.0 Si	0.1017(1)	0.5412(2)	0.2749(1)	0.48(1)
Si(3)	1.0 Si	0.1116(1)	0.5456(2)	−0.0813(1)	0.48(1)
Na(1)	0.967 Na + 0.033 Ca	0.0	0.0	0.0	1.40(4)
Na(2)	0.967 Na + 0.033 Ca	0.0705(2)	−0.0079(6)	0.1712(1)	1.55(4)
O(1)	1.0 O	0.9958(2)	0.3361(7)	0.0822(2)	0.74(4)
O(2)	1.0 O	0.1705(2)	0.2995(8)	0.1086(2)	0.91(4)
O(3)	1.0 O	0.1179(2)	0.3565(7)	−0.0147(1)	0.78(4)
O(4)	1.0 O	0.1024(3)	0.7672(7)	0.0674(2)	0.92(4)
O(5)	1.0 O	0.0	0.642(1)	0.25	0.71(5)
O(6)	1.0 O	0.1768(2)	0.7139(7)	0.2338(1)	0.83(4)
O(7)	1.0 O	0.1171(2)	0.6500(7)	0.3534(1)	0.72(4)
O(8)	1.0 O	0.1157(3)	0.2395(7)	0.2720(2)	1.07(5)
O(9)	1.0 O	0.1854(2)	0.2275(7)	0.4180(2)	0.95(4)

[12] that only Na atoms are present in the Na(1) octahedra and that the octahedral coordination about Na(2) is distorted, whereas Bakakin *et al.* [11] assumed the incorporation of Mn^{2+} cations into the Na(1) polyhedron and considered the Na(2) polyhedron as an eight-vertex polyhedron.

The structure-genetic characteristic features of crystallization of raite, manganonordite-(Ce), and ferronordite-(Ce). Mineralogical geochemistry of Mn in high-alkaline pegmatites. Discoveries of raite, representatives of the nordite family, varennesite, and other Mn-minerals related to derivatives of high-alkaline rocks from the Lovozero massif and the Saint-Amable sill (Quebec), which are rather similar in the mineral composition, made it possible to reveal a number of characteristic features of the mineralogical geochemistry of manganese in these formations.

The evolution of high-agpaitic magmatic and, particularly, postmagmatic (pegmatitic) systems in the above complexes and analogous alkaline complexes from Khibiny (the Kola Peninsula), Illimaussaq (South-West Greenland), and Saint-Elier (Quebec) is characterized by the so-called alkalinity wave. The activity of alkalis, primarily, of sodium, increases at the early stages and decreases at the late stages [16]. The role of water in processes of mineral formation increases with a decrease in temperature, and the late stages of the pegmatite formation can be considered virtually as hydrothermal. The most high-alkaline and, at the same time, high-temperature (400–450°C) pegmatites are those containing ussingite $Na_2AlSi_3O_8OH$ as the major mineral. These pegmatites are widespread in the Lovozero massif. It is these pegmatites in which all minerals of the nordite family were found. The highest alkalinity and a rather high temperature are responsible for the formation of anhydrous and low-water Mn-minerals with a lower degree of condensation of the silicon–oxygen complexes in ussingite pegmatites. In addition to nordites containing the $[Si_6O_{17}]$ tetrahedral ribbons, serandite $HNa(Mn,Ca)_2[Si_3O_9]$ containing the $[Si_3O_9]$ tetrahedral chains and ring silicates, such as kazakovite $Na_6MnTi[Si_6O_{18}]$ and steenstrupine-(Ce) $Na_{14}Ce_6(Mn,Fe)_4(Zr,Th)(OH)_2(PO_4)_6[Si_6O_{18}]_2 \cdot 3H_2O$, are also abundant in these pegmatites. With a decrease in temperature, the ussingite paragenesis changes to natrolite or analcime paragenesis, which are somewhat less alkaline and in which hydrous minerals play a substantially more significant role. At this stage, the essentially hydrous Na,Mn-silicates possessing more complicated silicon–oxygen complexes are raite, varennesite, shafranovskite $(Na,K)_6Mn_3^{2+}Si_9O_{24} \cdot 6H_2O$, and zakharovite $Na_4Mn_5^{2+}Si_{10}O_{24}(OH)_6 \cdot 6H_2O$. Note that, in minerals formed at this stage, Mn^{2+} cations are also constituents of Ti(Nb)-silicates with mixed layers. For example, the Yubileinaya pegmatite lode is typified by the presence of a Mn-analog of barytolamprophyllite of

Table 6. Interatomic distances (Å) in the structure of manganonordite-(Ce)

Sr polyhedron		*TR* polyhedron		Mn^{2+} tetrahedron	
Sr–O(2)	2.578(3) × 2	*TR*–O(6)	2.493(3) × 2	Mn^{2+}–O(2)	1.976(3) × 2
O(3)	2.757(3) × 2	O(7)	2.714(3) × 2	O(6)	2.000(3) × 2
O(4)	2.610(3) × 2	O(8)	2.499(3) × 2		
O(9)	2.561(3) × 2	O(9)	2.468(3) × 2		
	⟨2.626⟩		⟨2.563⟩		⟨1.988⟩
Na(1) octahedron				Na(2) octahedron	
Na(1)–O(1)	2.387(3) × 2			Na(2)–O(1)	2.685(4)
O(3)	2.531(3) × 2			O(2)	2.433(4)
O(4)	2.338(3) × 2			O(4)	2.463(4)
				O(5)	2.652(4)
				O(6)	2.492(4)
				O(8)	2.418(4)
	⟨2.418⟩				⟨2.524⟩
Si(1) tetrahedron		Si(2) tetrahedron		Si(3) tetrahedron	
Si(1)–O(1)	1.662(3)	Si(2)–O(5)	1.635(2)	Si(3)–O(1)	1.649(3)
O(2)	1.601(3)	O(6)	1.612(3)	O(7)	1.647(3)
O(3)	1.682(3)	O(7)	1.671(3)	O(7)	1.651(3)
O(1)	1.577(3)	O(8)	1.579(3)	O(9)	1.578(3)
	⟨1.630⟩		⟨1.624⟩		⟨1.631⟩
O(1)–O(2)	2.596(4)	O(5)–O(6)	2.584(2)	O(1)–O(3)	2.614(3)
O(3)	2.614(4)	O(7)	2.654(2)	O(7)	2.624(3)
O(4)	2.725(4)	O(8)	2.708(4)	O(9)	2.659(4)
O(2)–O(3)	2.573(2)	O(6)–O(7)	2.534(3)	O(3)–O(7)	2.616(2)
O(4)	2.732(4)	O(8)	2.721(4)	O(9)	2.705(4)
O(3)–O(4)	2.682(3)	O(7)–O(8)	2.667(4)	O(7)–O(9)	2.716(4)
	⟨2.654⟩		⟨2.645⟩		⟨2.656⟩

composition $Na_6Ba_3MnTi_6Si_8O_{24}(F,OH)_2$, whereas the Shkatulka pegmatite at the Alluaiv mountain (the Lovozero massif) and the Saint-Amable massif are typified by the presence of shkatulkalite $Na_{10}MnTi_3Nb_3(Si_2O_7)_6(OH)_2F \cdot 12H_2O$. The subsequent evolution of the mineral-forming system is characterized by a substantial decrease in the activity of alkalis, which leads to a change in the mineral forms of manganese. At this stage, alkali-free Mn-silicates, namely, yofortierite and Mn-sepiolite, which contain layers of (Si,O) tetrahedra and H_2O molecules located within interlayer cavities, as well as X-ray- amorphous hydrous Mn^{2+}, Mn^{3+}-silicate neotocite $(Mn,Fe)SiO_3NH_2O$, are formed under rather low-temperature hydrothermal conditions. At the final stage, which is the lowest-temperature (~50°C) hydrothermal stage that borders the hypergene one, oxide phases of manganese, namely, todorokite, pyrolusite, psilomelane, birnessite, and cryptomelane, are formed. These minerals contain Mn^{4+}, which is unambiguously indicative of oxidizing conditions prevailing at this stage.

This diversity of pegmatite and hydrothermal manganese minerals is typical primarily of the Lovozero massif, whose rocks are enriched with this element to a greater extent than those of agpaitic complexes from the Khibiny and Illimaussaq deposits [16]. Apparently, the reason why own manganese minerals appear primarily at late stages is that the lability of manganese under conditions of high alkalinity is larger than those of iron and magnesium. In the minerals of the latter elements (pyroxenes and, particularly, amphiboles), manganese is dissipated at the magmatic and early-pegmatitic stages. It is not inconceivable that Mn is separated from Fe in high-alkaline pegmatites, because at this stage, readily oxidized iron exists, for the major part, in the trivalent state, whereas manganese still retains the divalent state. This is clearly exemplified by paragenesis of aegirine $NaFeSi_2O_6$ and magnesioarfvedsonite $Na_3(Mg,Fe_2+)_4Fe^{3+}[Si_8O_{22}](OH)_2$ in the Lovozero peg-

Table 7. Interatomic distances (Å) in the structure of ferronordite-(Ce)

Sr polyhedron		*TR* polyhedron		Fe^{2+} tetrahedron	
Sr–O(2)	2.581(4) × 2	*TR*–O(6)	2.501(3) × 2	Fe^{2+}–O(2)	1.973(4) × 2
O(3)	2.761(4) × 2	O(7)	2.727(3) × 2	O(6)	1.990(4) × 2
O(4)	2.609(4) × 2	O(8)	2.495(4) × 2		
O(9)	2.566(4) × 2	O(9)	2.463(4) × 2		
	⟨2.629⟩		⟨2.546⟩		⟨1.981⟩
Na(1) octahedron				Na(2) octahedron	
Na(1)–O(1)	2.391(3) × 2			Na(2)–O(1)	2.684(4)
O(3)	2.533(4) × 2			O(2)	2.436(5)
O(4)	2.333(4) × 2			O(4)	2.456(5)
				O(5)	2.666(4)
				O(6)	2.498(5)
				O(8)	2.425(5)
	⟨2.419⟩				⟨2.527⟩
Si(1) tetrahedron		Si(2) tetrahedron		Si(3) tetrahedron	
Si(1)–O(1)	1.659(4)	Si(2)–O(5)	1.636(2)	Si(3)–O(1)	1.669(4)
O(2)	1.606(4)	O(6)	1.627(4)	O(3)	1.650(4)
O(3)	1.659(4)	O(7)	1.674(4)	O(7)	1.650(4)
O(4)	1.586(4)	O(8)	1.581(4)	O(9)	1.590(4)
	⟨1.634⟩		⟨1.629⟩		⟨1.639⟩
O(1)–O(2)	2.587(5)	O(5)–O(6)	2.603(4)	O(1)–O(3)	2.614(5)
O(3)	2.614(5)	O(7)	2.662(3)	O(7)	2.638(5)
O(4)	2.734(5)	O(8)	2.711(5)	O(9)	2.679(5)
O(2)–O(3)	2.582(5)	O(6)–O(7)	2.549(5)	O(3)–O(7)	2.622(5)
O(4)	2.746(5)	O(8)	2.725(5)	O(9)	2.722(5)
O(3)–O(4)	2.694(5)	O(7)–O(8)	2.676(5)	O(7)–O(9)	2.727(5)
	⟨2.659⟩		⟨2.654⟩		⟨2.667⟩

matites with Mn^{2+}-silicates. The incorporation of Mn^{2+} ions into minerals isomorphously with Fe^{3+} is substantially more hindered as compared to Fe^{2+} due to the difference in the ionic radii, and manganese is forced to separate with the formation of own phases. The evolution of mineral forms of manganese demonstrates that the oxidation potential in the systems under consideration increases further when Mn^{2+}-silicates change with time for neotocite (Mn^{3+}) and, then, for oxide phases (Mn^{4+}).

In conclusion, let us consider the characteristic features of the M^{2+} cationic composition in minerals of the nordite family from various sources. Presently, nordites are found in pegmatites from three alkaline massifs, namely, from Lovozero, Khibiny (the Kola Peninsula), and Dara Pioz (Tadzhikistan). Nordite-(Ce) from Dara Pioz is most enriched in zinc. Nordites from Khibiny contain somewhat smaller amounts of Zn, whereas samples from the Lovozero massif are substantially depleted in this element to the extent of forming Fe- and Mn-dominant phases [17]. This can be associated with the difference in the activity of S^{2-} in the pegmatite-forming process. It is known that, of three elements (Zn, Fe, and Mn), zinc possesses the highest affinity for sulfur. This is confirmed, in particular, by the fact that sphalerite is widespread in high-alkaline pegmatites, whereas iron sulfides are rare in occurrence, and manganese sulfides are virtually absent. The content of sulfides in the Dara Pioz pegmatites is very low, whereas Zn-silicates (minerals of the osumilite and willemite families) are abundant, which indicates the low activity of S^{2-} and accounts for the presence of purely zinc nordite. The content of sphalerite in ultraagpaitic pegmatites from Khibiny is somewhat larger; i.e., the activity of S^{2-} is higher. In these pegmatites, nordites with an intermediate Zn content are observed. In addition, another high-alkaline Zn-silicate kukisvumite is found in these pegmatites. In ussingite pegmatites from the Lovozero massif, sphalerite (cleiophane) is widely distributed playing sometimes the role of a minor rock-